

Synthesis, Crystal Structure, and EPR Studies of the Five-Coordinate $[\text{CuCl}_3(\text{H}_2\text{O})_2]^-$ Complex in $(\text{dabcoH}_2)_2\text{Cl}_3[\text{CuCl}_3(\text{H}_2\text{O})_2]\cdot\text{H}_2\text{O}$

Mingyi Wei and Roger D. Willett*

Chemistry Department, Washington State University, Pullman, Washington 99164

Received March 14, 1996[⊗]

The compound $(\text{dabcoH}_2)_2\text{Cl}_3[\text{CuCl}_3(\text{H}_2\text{O})_2]\cdot\text{H}_2\text{O}$, where dabco = 1,4-diazabicyclo[2.2.2]octane, has been synthesized, its structure has been determined by single-crystal structural analysis, and its properties have been investigated by powder and single-crystal EPR spectroscopy. The compound crystallizes in space group $Pnma$ at room temperature with unit cell dimensions of $a = 15.227(1)$ Å, $b = 7.467(1)$ Å, and $c = 20.166(2)$ Å with $Z = 4$. The structure was solved by the Patterson method and refined by full-matrix least-squares to $R = 4.3\%$ for 1681 observed reflections ($I > 2\sigma(I)$). The $[\text{CuCl}_3(\text{H}_2\text{O})_2]^-$ anion exists with a slightly distorted trigonal bipyramidal geometry in which the three Cl atoms lie in equatorial positions and the two water molecules are in axial positions. The distortion appears to be driven by the presence of $\text{N}-\text{H}\cdots\text{Cl}$ hydrogen bonds. The EPR spectra are also consistent with the presence of only a small distortion from trigonal bipyramidal geometry since $g_1 \sim g_2 > g_3 \approx 2.0$. Analysis of the geometry indicates the distortion consists primarily of a “negative” C_{2v} type. Analysis of the thermal parameters supports the supposition that the observed geometry corresponds to disorder over two “positive” C_{2v} distortions.

Introduction

Five-coordinate Cu(II) species with monodentate ligands are almost invariably distorted from regular trigonal bipyramidal (TBP), D_{3h} , or square pyramidal (SP), C_{4v} , symmetry.¹ The dearth of trigonal bipyramidal five-coordinated complexes has been rationalized by Reinen and co-workers on the basis of a pseudo-Jahn–Teller distortion of the idealized trigonal bipyramidal parent structure.² This involves a coupling between the electronic and vibrational wave functions that lowers the ground state energy. The understanding of the reason for these distortions is of significance because of the behavior observed for the CuCl_5^{3-} anion in $\text{M}(\text{NH}_3)_6\text{CuCl}_5$ salts.^{3,4} Here trigonal bipyramidal geometries are observed for the Cu(II) ion in the cubic room-temperature phase, but the anisotropic displacement parameters clearly indicate the presence of disorder for the anions. Below room temperature, a phase transition to a tetragonal phase occurs, in which distorted square pyramidal geometries exist. EPR data are temperature dependent below the phase transition temperature. Reinen et al. have argued that the room-temperature phase contains a time average of three square pyramidal species, but this has been disputed.

The interpretation revolves about the shape of the “Mexican hat” potential predicted by the pseudo-Jahn–Teller effect. For the idealized trigonal bipyramidal geometry, interaction of various normal vibration modes with electronic wave functions can lead to a mixing of excited state wave functions into the ${}^2A'$ ground state. This can lead to minima in the potential surface corresponding to distortions of the trigonal bipyramidal

geometry. The depth and location of these minima depend upon the strength of the coupling. Theory predicts a coupling with e' vibrations that lead to a distortion toward square pyramidal geometry. The presence of lattice strains due to anisotropic interactions with surrounding species can lead to stabilization of one or more of the minima. Reinen's conjecture for the $\text{M}(\text{NH}_3)_6\text{CuCl}_5$ systems assumes the existence of three well-isolated potential minima, with the CuCl_5^{3-} ions locked in a given minimum up to the phase transition temperature. In the high-temperature phase, a restricted Berry-type rotation is assumed to occur. An alternative explanation involves a minimum-energy reorientation path that passes through the trigonal bipyramidal geometry.

In attempt to grow single crystals of $\text{HCuCl}_3(\text{dabco})_2$,⁵ in which Cu(II) has a trigonal bipyramidal geometry with equatorial distances $\text{Cu}-\text{Cl} = 2.375(2)$ Å and axial distances $\text{Cu}-\text{N} = 2.118(6)$ Å, we observed the formation of the complex $(\text{dabcoH}_2)_2\text{Cl}_3[\text{CuCl}_3(\text{H}_2\text{O})_2]\cdot\text{H}_2\text{O}$. Here dabco = 1,4-diazabicyclo[2.2.2]octane. In the latter compound the Cu(II) ion has a slightly distorted trigonal bipyramidal geometry with three Cl atoms lying on the equatorial positions and two water molecules on axial positions. This is one of the few examples of five-coordinated Cu(II) complexes with only monodentate ligands. Detailed analysis shows that the distortion of the $[\text{CuCl}_3(\text{H}_2\text{O})_2]^-$ anion in this salt corresponds primarily to a “negative” e' distortion. The question exists as to whether the observed distortion corresponds to a static distortion induced by lattice strains or to a dynamic average over two “positive” e' distortions. In this paper we report the synthesis, crystal structure, and EPR studies of $(\text{dabcoH}_2)_2\text{Cl}_3[\text{CuCl}_3(\text{H}_2\text{O})_2]\cdot\text{H}_2\text{O}$.

Experimental Section

Preparation of $(\text{dabcoH}_2)_2\text{Cl}_3[\text{CuCl}_3(\text{H}_2\text{O})_2]\cdot\text{H}_2\text{O}$. The compound was prepared by dissolving a 2:1 mixture of 1,4-diazabicyclooctane and copper chloride in a dilute HCl solution. Crystals of $(\text{dabcoH}_2)_2\text{Cl}_3[\text{CuCl}_3(\text{H}_2\text{O})_2]\cdot\text{H}_2\text{O}$ were grown by slow evaporation of the solution at room temperature. They were filtered off and air-dried.

(5) Vissat, B.; Rodier, P.; Khodadad, N.; Dung, N.-H. *Acta Crystallogr.* **1988**, C44, 263.

[⊗] Abstract published in *Advance ACS Abstracts*, September 15, 1996.

- (1) (a) Reinen, D.; Atanasov, M. *Chem. Phys.* **1991**, 155, 157. (b) Reinen, D.; Atanasov, M. *Chem. Phys.* **1989**, 27, 136.
- (2) Reinen, D.; Atanasov, M. *Magn. Reson. Rev.* **1991**, 31, 167 and references therein.
- (3) (a) Bernal, I.; Korp, J. D.; Schlemper, E. O.; Hussain, M. S. *Polyhedron* **1982**, 1, 365. (b) Aoyama, T.; Ohba, S.; Saito, Y.; Bernal, I. *Acta Crystallogr.* **1992**, C48, 246.
- (4) (a) Reinen, D.; Friebel, C. *Inorg. Chem.* **1984**, 23, 791. (b) Atanasov, M.; König, W.; Craubner, H.; Reinen, D. *New J. Chem.* **1993**, 17, 115. (c) Reinen, D.; Atanasov, M. *Chem. Phys.* **1989**, 136, 27. (d) Reinen, D.; Atanasov, M. *Chem. Phys.* **1991**, 155, 157.

Table 1. Parameters for the Data Collection and Structure Refinement of $(\text{dabcoH}_2)_2\text{Cl}_3[\text{CuCl}_3(\text{H}_2\text{O})_2]\cdot\text{H}_2\text{O}$

empirical formula	$\text{C}_{12}\text{H}_{30}\text{Cl}_6\text{CuN}_4\text{O}_3$	$T, ^\circ\text{C}$	23
crystal system	orthorhombic	space group	$Pnma$
$a, \text{\AA}$	15.2269(14)	λ (Mo $K\alpha$), \AA	0.710 73
$b, \text{\AA}$	7.4673(8)	ρ_{calc} , g cm^{-3}	1.607
$c, \text{\AA}$	20.166(2)	μ (Mo $K\alpha$), cm^{-1}	1.671
$V, \text{\AA}^3$	2293.0(4)	R_w^a , %	4.30
Z	4	R_w^b , %	10.30
fw	554.64		

$$^a R = \sum ||F_o| - |F_c|| / \sum |F_o|. \quad ^b R_w = \sum w(|F_o| - |F_c|)^2 / \sum |F_o|^2)^{1/2}.$$

Physical Measurements. Polycrystalline powder EPR spectra were recorded on a Varian E-3 X-band spectrometer at ambient temperature and at liquid-nitrogen temperature. The finely powdered sample was packed in a quartz tube. The magnetic field strength was calibrated with a DPPH sample. Single-crystal EPR spectra were measured at room temperature. EPR-suitable single crystals showing well-developed (001), (010), and (100) faces were oriented with a Siemens R3 diffractometer upgraded to P4 specifications. The spectra were measured at 15° intervals for rotations of the crystal about the normal to each crystal face.

DSC measurements were performed over the temperature range $-150^\circ\text{C} < T < 100^\circ\text{C}$ with a Perkin-Elmer Delta DSC7 instrument. Crystalline samples were ground and sealed in the sample pans. Helium gas (flow rate 40 kPa) was used as the purge gas. The scan rate of $10^\circ\text{C}/\text{min}$ was used for both calibration and data collection. There was a minor anomaly observed around -30°C . However, the heat flow was too small to definitely indicate the presence of any structural phase transition.

Crystal Structure Determination. The crystal structure of the title compound was determined by single-crystal X-ray methods at ambient temperature: A pale green crystal with dimensions $0.24 \times 0.25 \times 0.28$ mm was mounted on a thin glass fiber with 5 min epoxy glue, and room-temperature intensity data were collected on a Syntex P2₁ diffractometer upgraded to Siemens P4 specifications using graphite-monochromated molybdenum radiation ($\lambda(K\alpha) = 0.710 73 \text{\AA}$). A total of 2181 intensity data were collected for $3^\circ < 2\theta < 50^\circ$. The data sets were reduced using the XSCANS program⁶ provided by Siemens and corrected for Lorentz and polarization effects. Empirical absorption corrections based on ψ scans were applied to the data. Three reference reflections were measured every 97 reflections and showed no decrease during the data collection time. Unit cell parameters were refined by a least-squares fitting procedure using 25 machine-centered reflections. A summary of the crystal parameters and details concerning the diffraction intensity data collection are given in Table 1.

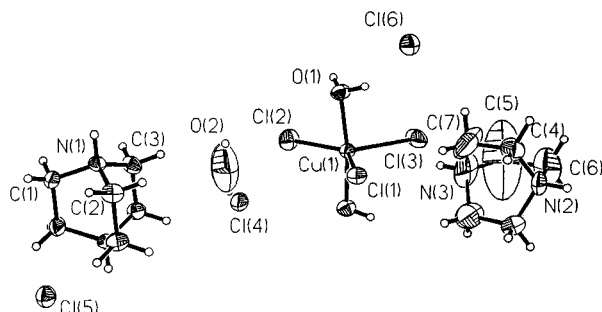
The structure was solved with SHELXS-90 crystallographic software^{7a} using the routine TREF command. The structure refinement was carried out with SHELXL-92 crystallographic software.^{7b} The non-hydrogen atoms were refined with anisotropic thermal parameters. Hydrogen atom positions of the dabcoH_2^{2+} cations were calculated and fixed at their calculated positions during the refinement. A fixed temperature factor of $U = 0.080 \text{\AA}^2$ was applied to the hydrogen atoms. The hydrogen atom positions of the water molecules were able to be located from Fourier difference maps and then refined with isotropic temperature factors. Full-matrix least-squares refinement on F^2 , based on 1681 observed reflections ($I > 2\sigma(I)$) and 149 variables, converged with $R = 0.043$ and $R_w = 0.103$. A final difference Fourier map showed no residual density outside the limits of -1.1 and $+1.2 \text{ e \AA}^{-3}$. Final positional parameters and equivalent isotropic thermal parameters are given in Table 2.

Another crystal with dimensions $0.18 \times 0.2 \times 0.4$ mm was used for low-temperature data collection at -42°C . The low-temperature intensity data were collected on a Siemens R3 diffractometer upgraded to P4 specification using graphite-monochromated copper radiation ($\lambda(K\alpha) = 1.541 78 \text{\AA}$). Temperature was controlled by a Siemens LT-2 device and calibrated by placing a small iron-constantan thermocouple

Table 2. Fractional Atomic Coordinates and Isotropic Thermal Parameters (\AA^2) for $(\text{dabcoH}_2)_2\text{Cl}_3[\text{CuCl}_3(\text{H}_2\text{O})_2]\cdot\text{H}_2\text{O}$

atoms	x	y	z	U_{eq}^a
Cu(1)	0.19317(5)	0.2500	0.67424(3)	0.0259(2)
Cl(1)	0.34291(9)	0.2500	0.70733(7)	0.0310(4)
Cl(2)	0.12583(11)	0.2500	0.57061(8)	0.0434(4)
Cl(3)	0.11066(12)	0.2500	0.77527(9)	0.0539(5)
Cl(4)	0.50076(12)	0.2500	0.55543(7)	0.0424(4)
Cl(5)	0.95858(9)	0.2500	0.38449(6)	0.0312(4)
Cl(6)	0.25415(10)	-0.2500	0.78374(7)	0.0396(4)
O(1)	0.1971(2)	-0.0129(4)	0.6685(2)	0.0329(7)
O(2)	0.3068(8)	0.2500	0.4973(6)	0.155(7)
N(1)	0.5188(2)	0.0830(4)	0.35012(14)	0.0255(7)
C(1)	0.5246(3)	0.1479(5)	0.2799(2)	0.0368(10)
C(2)	0.5960(2)	0.1476(6)	0.3892(2)	0.0346(10)
C(3)	0.4357(2)	0.1482(6)	0.3813(2)	0.0326(9)
N(2)	0.3712(3)	0.2500	0.9781(2)	0.0387(13)
N(3)	0.3041(5)	0.2500	0.8679(3)	0.086(3)
C(4)	0.4001(4)	0.0887(6)	0.9420(2)	0.0530(13)
C(5)	0.2413(7)	0.2500	0.9180(7)	0.302(19)
C(6)	0.2748(5)	0.2500	0.9863(5)	0.089(4)
C(7)	0.3596(7)	0.0935(9)	0.8760(3)	0.134(4)

$$^a U_{\text{eq}} = 1/3 \text{tr}[\mathbf{U}_{ij}].$$

**Figure 1.** ORTEP drawing of $(\text{dabcoH}_2)_2\text{Cl}_3[\text{CuCl}_3(\text{H}_2\text{O})_2]\cdot\text{H}_2\text{O}$, showing the atomic numbering and thermal ellipsoids at the 50% probability level.

at the crystal position. A total of 1820 intensity data were collected for $3^\circ < 2\theta < 110^\circ$. The XPREP program^{7a} was used to determine the space group. The statistical $|E^*E - 1|$ value dropped from 0.927 at room temperature to 0.877 (expected: 0.968 for a centrosymmetric space group and 0.736 for a noncentrosymmetric space group). Attempts were made to refine the low-temperature structure in both the centrosymmetric $Pnma$ and the noncentrosymmetric $Pna2_1$ space groups. Unreasonable thermal parameters were observed for the pseudocentrosymmetric structure. However the other structural parameters remained almost unchanged, especially for the geometry of the $[\text{CuCl}_3(\text{H}_2\text{O})_2]^-$ anion.

Results

Description of the Structure. The asymmetric unit of the crystal of the title compound consists of two dabcoH_2^{2+} cations, three Cl^- anions that are hydrogen-bonded to the dabcoH_2^{2+} cations, a discrete $[\text{CuCl}_3(\text{H}_2\text{O})_2]^-$ anion, and one lattice water molecule. Each copper(II) atom lies on a mirror plane in the crystal and is coordinated by three Cl^- anions and two molecules of water. The coordination geometry around Cu(II) is best described as distorted trigonal bipyramidal with two oxygen atoms occupying the axial positions. An illustration of the structure of the $[\text{CuCl}_3(\text{H}_2\text{O})_2]^-$ anion, including the atomic labeling scheme, is given in Figure 1. The bond distances and bond angles about the copper(II) ions are listed in Table 3.

The trigonal plane of the anion, composed of the atoms Cu(1), Cl(1), Cl(2), and Cl(3), sits on a crystallographic mirror plane. The O(1)–Cu(1)–O(1a) angle of $172.5(2)^\circ$ is not much different from 180° expected for ideal TBP geometry. The trigonal angles (between Cl(1), Cl(2), and Cl(3)) are inequivalent. The

(6) XSCANS program (1992), version 2.0a, Siemens Analytical X-ray Instruments Inc., Madison, WI.

(7) (a) Sheldrick, G. M. SHELXS-90 program. (b) Sheldrick, G. M. SHELXL-92 program.

Table 3. Bond Lengths (Å) and Bond Angles (deg) for the [CuCl₃(H₂O)₂]⁻ Anion in (dabcoH₂)₂Cl₃[CuCl₃(H₂O)₂]·H₂O

Distances			
Cu(1)—O(1)	1.967(3)	Cu(1)—Cl(2)	2.328(2)
Cu(1)—Cl(1)	2.376(2)	Cu(1)—Cl(3)	2.394(2)
Angles			
O(1)—Cu(1)—O(1)	172.5(2)	Cl(2)—Cu(1)—Cl(1)	132.45(6)
O(1)—Cu(1)—Cl(1)	89.28(10)	Cl(2)—Cu(1)—Cl(3)	122.20(7)
O(1)—Cu(1)—Cl(2)	87.76(10)	Cl(1)—Cu(1)—Cl(3)	105.34(7)
O(1)—Cu(1)—Cl(3)	93.75(9)		

Cl(1)—Cu(1)—Cl(2) angle is increased to 132.45(6)° from the idealized 120°, whereas the Cl(1)—Cu(1)—Cl(3) angle is decreased to 105.34(7)°. The Cu(1)—O(1) bond length is 1.967(3) Å and the mean Cu—Cl bond distance is 2.365(2) Å. The largest deviation comes from Cu(1)—Cl(2) bond length (2.328(2) Å), which is significantly shorter than the other two bond lengths (Cu(1)—Cl(1) = 2.375(2) Å and Cu(1)—Cl(3) = 2.393(2) Å). The O(1) atom is tipped toward the shortest of the three Cu—Cl bonds, with Cl(2)—Cu—O(1) = 87.76(10)°. The Cu—Cl bond distances are comparable to the equatorial Cu—Cl distances observed in the time-averaged trigonal bipyramidal CuCl₅³⁻ anion in Co(NH₃)₆CuCl₅³⁻ and somewhat longer than the basal Cu—Cl distances in the slightly distorted square pyramidal coordination geometry.⁸

There are two crystallographically independent dabcoH₂²⁺ cations. Both of them have mirror plane symmetry. However, one dabcoH₂²⁺ cation (hereafter called dabco1) has the mirror plane that bisects the three C—C bonds while the other dabcoH₂²⁺ cation (hereafter called dabco2) has the mirror plane oriented so that two N atoms and two C atoms are located on it. As seen from the ORTEP plot in Figure 1, the displacement ellipsoids for C(6) and C(7), which sit on the mirror, are very large, implying disorder. This would indicate that the N—C—C—N linkages are nonplanar in this cation, and the torsional disorder occurs about the N—N axis. The rigid-body motion analyses performed using a generalized TLS procedure⁹ given in the SHELXTL-PLUS program for both dabco1 and dabco2 cations also support the existence of disorder in the dabco2 cation. The root-mean-square deviations between the observed displacement parameters and those calculated from TLS were compared with the average experimental standard deviations over all tensor components of all atoms in the cation. The calculated root-mean-square deviation for the dabco2 cation is 10 times larger than the observed one, while for the dabco1 cation they are of the same order of magnitude.

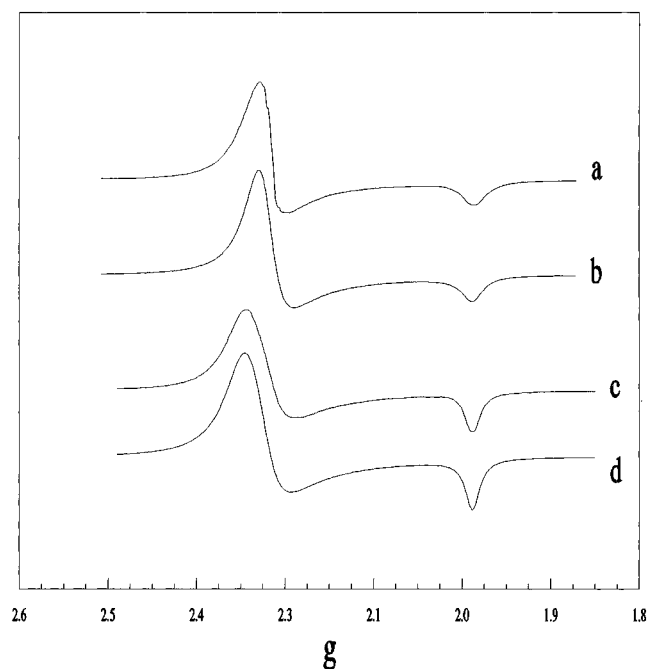
The average C—N bond lengths of the dabco1 and dabco2 cations are 1.496(5) and 1.449(9) Å, respectively. As the result of the disorder in the dabco2 cation, the N(3)—C(5) distance of 1.392(15) Å is shorter than the other C—N distances. The average C—C bond lengths of the dabco1 and dabco2 cations are 1.525(8) and 1.47(2) Å, respectively. Again the C—C distance is shorter in the dabco2 cation due to the disorder.

There is an extensive and strong three-dimensional hydrogen-bonding network among the dabcoH₂²⁺ cations, the water molecule, the [CuCl₃(H₂O)₂]⁻ anion, and the Cl⁻ anions. The possible hydrogen-bonding contacts are listed in Table 4. The shortest interaction is N(2)—H(2)···Cl(5). The other hydrogen bonds are weaker, due to the formation of bifurcated or trifurcated bonds with angles deviating from 180°. Note that for the CuCl₃(H₂O)₂⁻ anion, only Cl(1) and Cl(3) are involved

Table 4. Hydrogen-Bonding Distances and Angles

atom 1—atom 2···atom 3 ^a	2—3, Å	1—3, Å	∠1—2—3, deg
N(1)—H(1)···Cl(1) ^a	2.881	3.458	123.3
N(1)—H(1)···Cl(3) ^b	2.944	3.513	122.7
N(1)—H(1)···Cl(4) ^a	2.495	3.145	129.5
N(2)—H(2)···Cl(5) ^c	2.175	3.075	179.2
N(3)—H(3)···Cl(1)	2.618	3.291	132.2
N(3)—H(3)···Cl(3)	2.763	3.486	138.2
O(1)—H(11)···Cl(5) ^b	2.375	3.145	163.1
O(2)—···Cl(4) [?]		3.121	
O(2)—···Cl(4) [?]		3.180	

^a Superscripts refer to the following transformations of the coordinates: (a) 1 - x, -y, 1 - z; (b) 0.5 - x, -y, 0.5 + z; (c) -0.5 + x, y, 1.5 - z.

**Figure 2.** EPR powder spectra of (dabcoH₂)₂Cl₃[CuCl₃(H₂O)₂]·H₂O: (a) room temperature, experimental; (b) room temperature, simulated; (c) liquid-N₂ temperature, experimental; (d) liquid-N₂ temperature, simulated.

in hydrogen bonding. This contributes to the deformation observed in the *D*_{3h} geometry, causing the Cu(1)—Cl(1) and the Cu(1)—Cl(3) bond distances to be longer than the Cu(1)—Cl(2) distance by 0.048 and 0.064 Å, respectively. The lattice water molecule is also involved in hydrogen bonding, as indicated by the distances O(2)···Cl(2) = 3.121 Å and O(2)···Cl(4) = 3.180 Å. The hydrogen atoms of the lattice water molecule did not refine into positions that favor the formation of hydrogen bonds. Because of the larger displacement parameters of the O(2) atom, the lattice water molecule may be disordered across the mirror plane.

EPR Studies. The powder EPR spectra of (dabcoH₂)₂Cl₃[CuCl₃(H₂O)₂]·H₂O at room temperature and liquid-nitrogen temperature are shown in Figure 2, along with the computer-simulated spectra. The spectra exhibit a nominal axial pattern in the solid state with the *g*_{||} value only slightly above 2.00 and *g*_⊥ ≈ 2.28. Simulation studies using the program POWFIT¹⁰ show these spectra to actually be rhombic with the crystal *g* values listed in Table 5.

The single-crystal EPR spectra were recorded at room temperature and X-band frequency at regular intervals of rotation

(8) (a) Antolini, L.; Marcotrigiano, G.; Menabue, L.; Pellacani, G. C. *J. Am. Chem. Soc.* **1980**, *102*, 1303. (b) Bonamartini-Corradi, A.; Battaglia, L. P.; Rubenacker, J.; Willett, R. D.; Grigereit, T. E.; Zhou, P.; Drumheller, J. E. *Inorg. Chem.* **1992**, *31*, 3859.
(9) Shoemaker, V.; Trueblood, K. N. *Acta Crystallogr.* **1968**, *B24*, 63.

(10) POWFIT EPR simulation software distributed by the Laboratory of Molecular Biophysics, National Institute of Environmental Health Sciences.

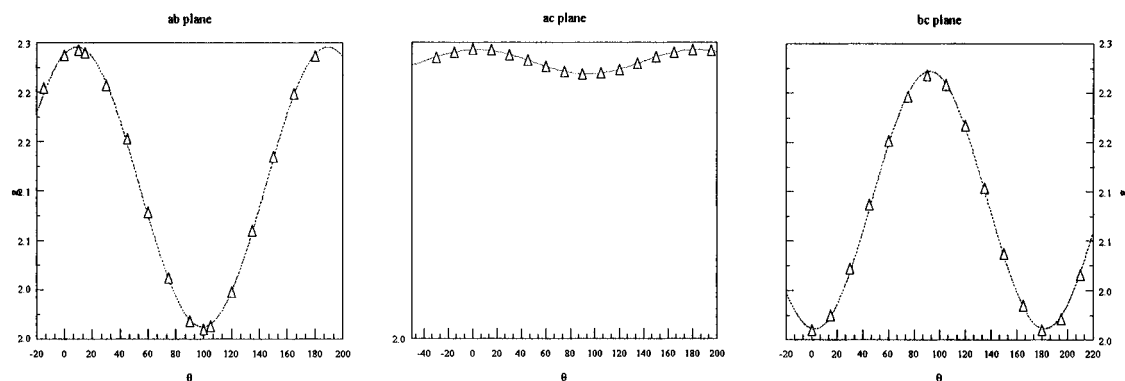


Figure 3. Angular dependencies of the g values for $(\text{dabcoH}_2)_2\text{Cl}_3[\text{CuCl}_3(\text{H}_2\text{O})_2]\cdot\text{H}_2\text{O}$ in the three crystallographic a , b , and c axes.

Table 5. Principal g Values for the $[\text{CuCl}_3(\text{H}_2\text{O})_2]^-$ Anion in $(\text{dabcoH}_2)_2\text{Cl}_3[\text{CuCl}_3(\text{H}_2\text{O})_2]\cdot\text{H}_2\text{O}$

	g_a	g_c	g_b
polycrystalline sample (room temperature)	2.294	2.264	2.010
polycrystalline sample (liquid- N_2 temperature)	2.294	2.280	2.010
single-crystal sample (rotation about a axis)		2.27	2.01
single-crystal sample (rotation about b axis)	2.29	2.27	
single-crystal sample (rotation about c axis)	2.29		2.01

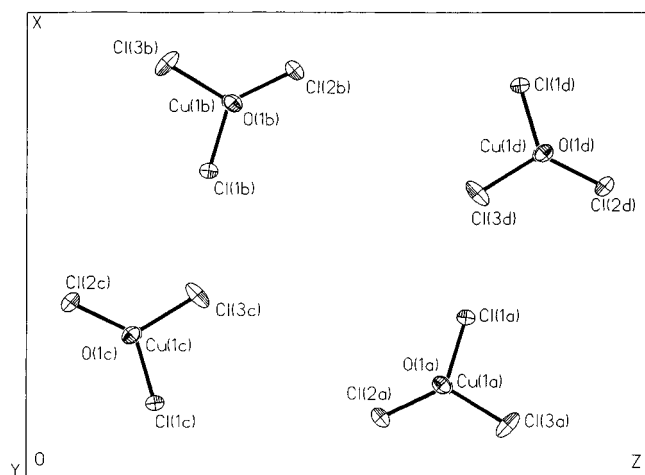


Figure 4. Projection of the four $[\text{CuCl}_3(\text{H}_2\text{O})_2]^-$ anions in the unit cell onto the (001) plane.

about the crystallographic a , b , and c axes. The angular dependence of the g values, along with the calculated g values, is shown in Figure 3. The principal g values of 2.01, 2.27, and 2.29 were obtained from the least-squares fitting¹¹ of the data and are listed in Table 5. The orientation of the $[\text{CuCl}_3(\text{H}_2\text{O})_2]^-$ anion is such that one of the principal g axes must be parallel to the crystal b axis and the other two must lie in the ac plane. The positions of the four $[\text{CuCl}_3(\text{H}_2\text{O})_2]^-$ anions in the unit cell are projected onto the ac plane (Figure 4). Two signals were expected in the single-crystal EPR experiment. However, only a single resonance was observed at all orientations, and thus the solid is probably not magnetically dilute enough for the EPR experiment to yield the molecular g values directly. It is reasonable to assume that the two differently oriented $[\text{CuCl}_3(\text{H}_2\text{O})_2]^-$ anions, which are separated by a distance of 8.204 Å, are exchange-coupled via the extensive hydrogen-bonding network.

It is desirable to know the molecular g values in order to characterize the extent of the distortion of the anion. It is possible to place limits on the molecular g values by analyzing the following equations which relate the crystal g values to the

Table 6. Variation of Molecular g Values as a Function of α from 0 to 40°

	α , deg								
	0	10	16.3 ^a	20	26.1 ^b	30	31.7 ^c	35	40
g_1	2.293	2.294	2.295	2.297	2.301	2.305	2.308	2.316	2.349
g_2	2.269	2.268	2.267	2.265	2.261	2.257	2.254	2.246	2.211

^a Parallel to the Cu(1)–Cl(1) bond direction. ^b Parallel to the Cu(1)–Cl(2) bond direction. ^c Parallel to the Cu(1)–Cl(3) bond direction.

molecular g values.¹² Here the directions of the principal g values (g_a , g_b , g_c) are labeled consistently with the crystallographic a , b , and c axes, and 2α is the angle between the two corresponding molecular g directions. The molecular g values, denoted by g_1 , g_2 , and g_3 ($g_1 > g_2 > g_3$), are related to the crystal g values by the relations

$$g_a = g_1 \cos^2 \alpha + g_2 \sin^2 \alpha$$

$$g_b = g_3$$

$$g_c = g_1 \sin^2 \alpha + g_2 \cos^2 \alpha$$

From these equations, we know that one of the principal g value (g_b) is equal to the molecular g value (g_3). The other two molecular g values (g_1 and g_2) can be calculated only if the angle α is known. There is no solution when α approaches 45°. Table 6 gives the g values as α is varied from 0 to 40°. Very reasonable g values ($g_1 < 2.32$ and $g_2 > 2.25$) are observed for α less than 35°. Within this angle range, g_1 can be chosen to be close to any Cu–Cl bond direction (Table 6). In particular, if the g tensor is assumed to be coincident with the pseudo- C_{2v} geometry (g_1 parallel to the Cu(1)–Cl(2) direction), one obtains $g_1 = 2.301$ and $g_2 = 2.261$.

Discussion

The geometries of five-coordinated copper complexes are quite varied. However, the more regular five-coordinate geometries of D_{3h} and C_{4v} symmetry are rarely seen. The predominance of the low-symmetry five-coordinated complexes has been rationalized by Reinen and co-workers on the basis of a pseudo-Jahn–Teller distortion along the $D_{3h} \leftrightarrow C_{4v}$ pathway.^{1b} There are only a few species that have geometries located along this idealized pathway. Most five-coordinated compounds adopt a so-called folded 4 + 1 coordination geometry.¹³ In this geometry, there are four short (normal) Cu–L bonds and one long (semicoordinate) Cu···L bond. The four short Cu–L bonds define two distinct *trans* L–Cu–L

(11) (a) Geusic, J. E.; Brown, L. C. *Phys. Rev.* **1958**, *112*, 64. (b) Billing, D. E.; Hathaway, B. J. *J. Chem. Phys.* **1969**, *50*, 2258.

(12) Billing, D. E.; Hathaway, B. J. *J. Chem. Phys.* **1969**, *50*, 1476. The equations used in this paper are a special case in which $\beta = \gamma = 90^\circ$.

(13) Blanchette, J.; Willett, R. D. *Inorg. Chem.* **1988**, *27*, 843.

angles, one typically lying between 155 and 175° and the other in the range 135–155°. Because of elongation of the axial Cu···L bond, the sum of the five Cu–L bonds is also usually larger than the sum anticipated for ideal trigonal bipyramidal or square pyramidal geometries.

The [CuCl₃(H₂O)₂][−] anion is an example of an isolated five-coordinated Cu(II) complex with nonchelating ligands. Unlike the case of most of five-coordinated copper complexes, there is no distinctively elongated Cu–Cl bond in the [CuCl₃(H₂O)₂][−] anion. The geometry of the [CuCl₃(H₂O)₂][−] anion cannot be described as the folded 4 + 1 type. Lacking a 2-fold axis, the geometry of the [CuCl₃(H₂O)₂][−] anion is obviously off of the $D_{3h} \leftrightarrow C_{4v} \leftrightarrow C_{2v}$ pathway. If the angular distortions from C_{2v} symmetry (the two angles adjacent to the shortest Cu–Cl bond, which should be equal for C_{2v} symmetry, are 132.45 and 122.20°) are ignored, the geometry of the [CuCl₃(H₂O)₂][−] anion can be regarded as another example of “reverse” geometry, which is only observed in Cu(terpy)(NCS)₂ and Cu(terpy)Br₂.¹⁴ In the latter pair, the reason for “negative” deviation (−ε′ displacement) is attributed to the strain characteristics of the terpy ligand. The strain in the [CuCl₃(H₂O)₂][−] anion may be due to the different σ-bonding strengths of the Cl and O atoms and/or the hydrogen bonds involved in the [CuCl₃(H₂O)₂][−] anion.

The rigid-body motion analyses for the [CuCl₃(H₂O)₂][−] anion was performed using a generalized TLS procedure.⁹ The root-mean-square deviations between the observed displacement parameters and those calculated from TLS was found to be 0.006. The average experimental standard deviation over all tensor components of all non-hydrogen atoms in the [CuCl₃(H₂O)₂][−] anion was found to be 0.0009. The results indicated that the rigid-body test is not satisfied. Further support for the non-rigid-body motion involved in the [CuCl₃(H₂O)₂][−] anion is that there is substantial electron residual (−1.1 and 1.2 e Å^{−3}) around Cl(3), the Cl that has fairly large displacement parameters. As pointed out by Reinen and co-workers,¹⁴ the “reverse” geometry could be the average of two elongated square pyramids. The magnitude and shape of the thermal ellipsoids for the chloride ions in the basal plane lead us to suspect that

there is disorder for the [CuCl₃(H₂O)₂][−] anion. If the observed geometry for the [CuCl₃(H₂O)₂][−] anion is the average of two elongated square pyramids, then the Cu–Cl bond distances for the C_{2v} geometry species would be approximately 2.23 Å for the pair of short bonds and 2.44 Å for the elongated bond. The disorder of the [CuCl₃(H₂O)₂][−] anion may imply a very shallow minimum on the potential surface, which compares well with theoretically calculated potential surfaces for five-coordinated Cu(II) complexes.¹ The small anomaly observed at −30 °C may be associated with the “freezing in” of this disorder.

Note Added in Proof. The ground state potential surface for the [CuCl₃(H₂O)₂][−] anion has been calculated in the angular overlap method approximation.¹⁵ The principal features include a single minimum corresponding to D_{3h} symmetry along with a considerable softening in the three directions corresponding to C_{2v} distortion pathways. This is in contrast to the case for the CuCl₅^{3−} anion where distinct minima are observed in those three directions. Prof. Atanasov has kindly pointed out that the observed distortions can be quantified by the following:

$$\text{stretching modes: } Q_{\epsilon} = Q_{\xi} = 0.034 \text{ \AA}$$

$$\text{bending modes: } Q_{\epsilon} = 0.067 \text{ \AA}, Q_{\xi} = 0.458 \text{ \AA}$$

The observed distortion is the first example of an isolated Cu(II) complex with primarily a Q_{ξ} type distortion. The combination of distortions corresponds to the stabilization of one of the ±120° pathways on the potential surface, corresponding to the elongation of the Cu–Cl(3) bond. The observed distortion thus represents an interesting interplay between hydrogen-bonding effects and weak vibronic coupling.

Acknowledgment. This work was supported by NSF Grant No. CHE-9113409.

Supporting Information Available: Tables S1–S4, listing crystallographic and refinement parameters, cation bond distances and bond angles, anisotropic thermal parameters, and H atom positions for (dabcoH₂)₂Cl₃[CuCl₃(H₂O)₂]·H₂O (6 pages). Ordering information is given on any current masthead page.

IC9602862

(14) Arriortua, M. I.; Mesa, J. L.; Rojo, T.; Debaerdemaeker, T.; Beltran-Porter, D.; Stratemeier, H.; Reinen, D. *Inorg. Chem.* **1988**, *27*, 2976.

(15) Wei, M.; Willett, R. D.; Atanasov, M. Z. *Phys. Chem.*, in press.